The Journal of Chemical Physics

Communication: Appearance of undershoots in start-up shear: Experimental findings captured by tumbling-snake dynamics

Cite as: J. Chem. Phys. **146**, 161101 (2017); https://doi.org/10.1063/1.4982228
Submitted: 29 March 2017 . Accepted: 13 April 2017 . Published Online: 25 April 2017

Pavlos S. Stephanou, Thomas Schweizer, and Martin Kröger

Communication: Appearance of undershoots in start-up shear: Experimental findings captured by tumbling-snake dynamics

Pavlos S. Stephanou,[1,a)] Thomas Schweizer,[2] and Martin Kröger[2,b)]
[1]*Department of Mathematics and Statistics, University of Cyprus, P.O. Box 20537, 1678 Nicosia, Cyprus*
[2]*Department of Materials, Polymer Physics, ETH Zürich, CH-8093 Zürich, Switzerland*

(Received 29 March 2017; accepted 13 April 2017; published online 25 April 2017)

Our experimental data unambiguously show (i) a damping behavior (the appearance of an undershoot following the overshoot) in the transient shear viscosity of a concentrated polymeric solution, and (ii) the absence of a corresponding behavior in the transient normal stress coefficients. Both trends are shown to be quantitatively captured by the bead-link chain kinetic theory for concentrated polymer solutions and entangled polymer melts proposed by Curtiss and Bird, supplemented by a non-constant link tension coefficient that we relate to the nematic order parameter. The observed phenomena are attributed to the tumbling behavior of the links, triggered by rotational fluctuations, on top of reptation. Using model parameters deduced from stationary data, we calculate the transient behavior of the stress tensor for this "tumbling-snake" model after startup of shear flow efficiently via simple Brownian dynamics. The unaltered method is capable of handling arbitrary homogeneous flows and has the promising capacity to improve our understanding of the transient behavior of concentrated polymer solutions. *Published by AIP Publishing.* [http://dx.doi.org/10.1063/1.4982228]

It is today well accepted that the dynamical behavior of entangled polymer melts and concentrated solutions is triumphantly predicted by an effective medium theory, the tube/reptation model proposed by Doi, Edwards, and de Gennes.[1–3] In essence, the dynamics of a high-molecular-weight chain is confined within an effective mean-field tube defined by the topological constraints imposed by surrounding chains. Thus, escape from the tube can only occur via a curvilinear diffusion (termed reptation) along the tube's centerline after an amount of time approximately equal to the reptation or disengagement time, τ_d.[1–5] Numerical algorithms able to extract the primitive path network from lower-level simulations have provided the means to study both the entanglement statistics[6–9] and dynamics,[10–13] providing invaluable information to reassess modern tube/reptation models.[14–17] Overall, both experiments and simulations have unambiguously documented that the tube/reptation framework today stands as a powerful tool necessary to understand the linear viscoelastic (LVE) behavior of entangled polymer melts and solutions.

Under flow conditions, as illustrated by Doi-Edwards (DE),[2,18–20] its treatment requires the solution of a Fokker-Planck (FP) equation for the single-link distribution function, $f(\sigma, \mathbf{u}, t)$, which describes the probability that at time t a chain segment at reduced contour position $\sigma \in [0, 1]$ along the chain is oriented in the direction $\mathbf{u}$, while $\mathbf{u}$ and σ are independent dynamical variables. Curtiss and Bird (CB), a few years after DE, employed a phase-space formulation for the kinetic theory of undiluted polymers[21] to develop a kinetic theory for polymer melts and concentrated solutions composed of multi-bead chains[21–25] that we coin as the "tumbling-snake" model.

The assumptions of this model are completely different from those made by DE.[21,26] An additional term, corresponding to a rotational Brownian contribution with a parameter $\varepsilon' \in [0, 1]$ controlling its significance, is added to the FP equation.[21,26] The tumbling-snake model includes a contribution in the extra stress tensor containing the fourth moment of f that arises from the anisotropy of the friction tensor within their kinetic theory derivation and is controlled by the link tension coefficient $\varepsilon \in [0, 1]$. In addition, the stress tensor contains two contributions related to the plain and $\sigma(1-\sigma)$-weighted second moment of f, whose relative significance is given by ε'. The DE model is recovered as a limiting case of the tumbling-snake model (when $\varepsilon = \varepsilon' = 0$), and the time constant of the tumbling-snake model, denoted as λ, is proportional to the reptation time, $\lambda = \pi^2 \tau_d$. CB and their co-workers had solely employed the analytically tractable non-tumbling limit of their model, with $\varepsilon' = 0$ and $\varepsilon > 0$.[21–25,27] The tumbling-snake model involving non-vanishing ε and ε' has since then been apparently overlooked.

As two of us have demonstrated very recently,[26] the tumbling-snake model can readily be solved via Brownian dynamics (BD). We have explicitly shown that the tumbling-snake model allows for a better description of more recent rheological data that exhibit power-law slopes larger than those predicted by the non-tumbling model. In this work, based on our experimental results that serve to test the nonequilibrium-dynamical properties, we are led to suggest an expression for the calculation of the link tension coefficient through the nematic order parameter,[28] $\varepsilon \sim S_2^2$ (see below for details).

There is accumulated evidence today revealing that under high-shear-rate startup experiments the time-dependent shear viscosity $\eta(t)$ exhibits a damped oscillatory behavior, in which $\eta(t)$ first overshoots and then undershoots the steady-state value before eventually reaching it.[29,30] Such evidence has

a)Author to whom correspondence should be addressed. Electronic mail: stefanou.pavlos@ucy.ac.cy
b)URL: http://www.complexfluids.ethz.ch.

only recently been brought to light since accurate rheological measurements at high shear rates have been, for quite some time, a challenge for rheologists due to edge fracture. This damping behavior seems to be more pronounced in polymer solutions rather than polymer melts. The reason for its appearance has thus far evaded a clear explanation. Such a behavior for $\eta(t)$ is predicted by a thermodynamically admissible reptation model,[31] although this work did not further elaborate as to which mechanism is responsible. More recently, Costanzo *et al.*[30] proposed that the reason for this trend is the tumbling of entangled polymer chains and accounted for this via a phenomenological modification to a tube-based model which allows for tumbling[32,33] to occur through the introduction of a "tumbling" function. In our present work, we account for this tumbling via the rotational Brownian contribution of the tumbling-snake model.

In this Communication, we present experimental data for all transient rheological properties of a polymer solution subjected to shear. The results unequivocally reveal the appearance of a damped oscillatory behavior of $\eta(t)$ and, within statistical uncertainty, absence of any oscillatory behavior in the transient first and normal stress coefficients, $\Psi_1(t)$ and $\Psi_2(t)$, respectively. Furthermore, motivated by the fact that such a damping behavior is known to occur in rigid rods,[34] we solve the tumbling-snake model for $\varepsilon' > 0$ in startup shear flow (using BD simulations) and show that it does bear the adequate capacity to capture these observations.

The nearly monodisperse polystyrene (PS) solution was prepared and characterized as described in Section A of the supplementary material. The rheological measurements were performed at 30 °C with a partitioned plate setup, connected to two measuring motors, that provides two normal forces and two torque signals, one for the entire sample and one for the inner partition. Transient rheological measurements are provided for $\eta(t)$ (Fig. 1) and $\Psi_1(t)$ and $\Psi_2(t)$ (Fig. 2) for various shear rates $\dot\gamma$, whereas their steady-state values are collected in Fig. S2 of the supplementary material. As the statistical uncertainties for the transient measurements are difficult to quantify, we depict in Figs. 1 and 2, their lower limits, the steady-state statistical uncertainty, at the last transient data point.

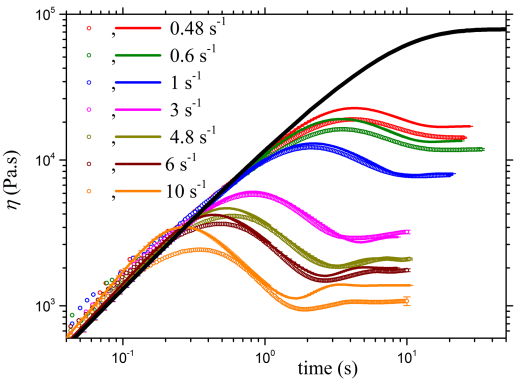

FIG. 1. Comparison of transient shear viscosity $\eta(t)$ PS solution measurements (symbols) with the tumbling-snake model predictions (lines) for different shear rates $\dot\gamma$. The added statistical uncertainties are those calculated at steady-state conditions. System parameters: $N = 3Z = 42$ (since $Z \approx 14$, see Table S-I of the supplementary material), $\varepsilon_0 = 0.1$ (Fig. S2 of the supplementary material), $\varepsilon_0' \equiv (N-1)^2\varepsilon' = 1$, $G = 45$ kPa, and $\lambda = 105$ s (Fig. S1 of the supplementary material). The thick black line depicts the LVE envelope, Eq. (C11a) of the supplementary material.

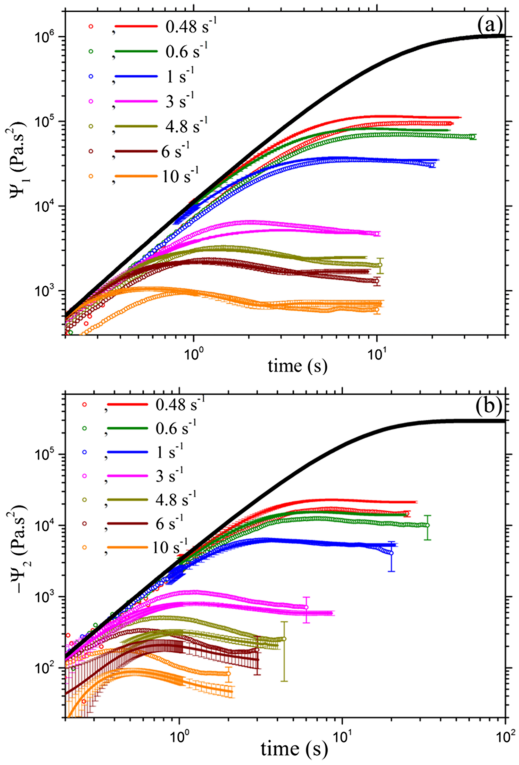

FIG. 2. Same as Fig. 1, using strictly identical parameters, but for the transient (a) first, $\Psi_1(t)$, and (b) second, $\Psi_2(t)$, viscometric function. Experimental data (symbols) versus theory (lines).

We unambiguously see that for $\dot\gamma \geq 1.6\ \text{s}^{-1}$ an undershoot occurs in $\eta(t)$ which deepens and whose position is shifted towards smaller times as $\dot\gamma$ increases. It should be noted that a PS polymer melt with almost the same number of entanglements ($Z \approx 16$) does not present any undershoots,[35] suggesting $\varepsilon' = 0$ for melts (see below for more details). The considerable hindrance for links to rotate in polymer melts as compared to the relative easiness in a dilute polymer solution may serve as the underlying reason. A negligible or vanishing ϵ' for melts is also in accord with our recent work[26] where we needed to employ an ε' parameter that decreased with increasing polymer concentration to successfully compare the tumbling-snake model predictions with steady-state shear viscosity data of an entangled DNA solution. Concerning $\Psi_1(t)$ and $\Psi_2(t)$ (Fig. 2), although some oscillations at large $\dot\gamma$ are indeed observed, their amplitudes are small and comparable to the statistical uncertainty; for this reason, our conclusion is that a damping behavior is not observable in these viscometric functions. Data are generally shown up to times where edge fracture sets in.

The LVE envelopes, presented in Figs. 1 and 2, are calculated analytically by considering a spherical harmonics expansion of the single-link distribution function around equilibrium, using the methods of Ref. 26 (see Section C of the supplementary material). Analytical expressions were also derived for the frequency-dependent storage and loss moduli (Section B of the supplementary material). We take the number of beads to be equal to $N = 3Z = 42$ since the number of entanglements is $Z \approx 14$ (see Table S-I of the supplementary material). The relation $N = 3Z$ is deduced by requiring

that the stress tensor expression of the tumbling-snake model when $\varepsilon' = \varepsilon = 0$ matches that of the DE model.[23,26,36] The values for the modulus, $G = 45$ kPa, and the relaxation time, $\lambda = 105$ s, were both obtained by fitting the storage and loss moduli (Fig. S1 of the supplementary material) and the $\eta(t)$ LVE envelope (Fig. 1) of the polymer solution under study. The choice $\varepsilon'_0 = \varepsilon'(N-1)^2 = 1$ is necessary so that the undershoots are comparable to those found in our experimental data.

Finally, concerning the link tension coefficient, we can deduce that it cannot be taken as a constant as originally considered by Bird *et al.*[21–25,27] At early times, the polymer chain would not have had enough time to respond to the applied flow field, and tension in each entanglement strand should be approximately equal to the equilibrium one, just like the DE model; this directly suggests that $\lim_{t\to 0}\varepsilon(t) = 0$ (see also Example 19.1-1 in Ref. 21). This reasoning is in accord with the fact that experimental data (Fig. 1) for $\eta(t \to 0)$ always approach zero instead of a finite non-zero value $\varepsilon G\lambda/90$, as predicted by the original CB model for a positive constant ε (see Ref. 24). In addition to this, $\Psi_2(t)$ is seen to change sign at small times when the link tension coefficient is treated as a constant.[24] On the other hand, a non-zero asymptotic value $\lim_{t\to\infty}\varepsilon(t)$ is needed to correctly capture the steady-state experimental data. However, the use of a finite, constant ε is known to lead to a violation of the stress-optic law,[37] which is expected to hold close to equilibrium (far away from equilibrium, the chain stretch becomes nonlinear and a failure of the stress-optic law is measured[38]). We thus have convincing evidence that the tumbling-snake model has to be used with a non-constant link tension coefficient.

In principle, we would expect the scalar link tension coefficient to be affected by S_4, the nematic scalar order parameter of the fourth rank orientation tensor,[28] as the corresponding contribution to the stress tensor involves this moment of f. Here we employ the simplest possible closure approximation, the so-called quadratic approximation $S_4 = S_2^2$,[28] involving the nematic order parameter S_2 of the 2nd moment $\langle\mathbf{uu}\rangle^{(1)}$ of f, $\langle\mathbf{uu}\rangle^{(1)} = \int_0^1 d\sigma \int d\mathbf{u} f(\sigma,\mathbf{u},t)\mathbf{uu}$ and propose an expression for the link-tension coefficient of the form $\varepsilon = \varepsilon_0 S_2^2$. The link-tension coefficient ε thus vanishes for an isotropic ensemble, approaches ε_0 for a fully aligned sample, and can be calculated from the anisotropic orientation tensor $\langle\mathbf{uu}\rangle^{(1)}_{\text{ani}} = \langle\mathbf{uu}\rangle^{(1)} - \frac{1}{3}\mathbf{I}$, where $\mathbf{I}$ is the unit tensor, via $S_2^2 = \frac{3}{2}\text{tr}\left(\langle\mathbf{uu}\rangle^{(1)}_{\text{ani}} \cdot \langle\mathbf{uu}\rangle^{(1)}_{\text{ani}}\right)$. This expression alleviates all drawbacks coming with the use of a constant ε: it vanishes at equilibrium, and its steady-state value increases with the imposed flow rate, which is the expected qualitative behavior. The value of ε_0 can be obtained from a comparison with the steady-state material functions (from Fig. S2 of the supplementary material, we obtain $\varepsilon_0 = 0.1$ for our data). By using this expression, we depict the transient link tension coefficient in Fig. 3 (in Fig. S2(d) of the supplementary material, we depict the steady-state ε). At early times, the link tension coefficient increases as $(\dot\gamma t)^2$. This can be shown by first expanding S_2 at small shear rates

$$\varepsilon = \frac{4}{75}\varepsilon_0(\dot\gamma\lambda)^2(\Gamma_1(0) - \Gamma_1(t))^2, \tag{1}$$

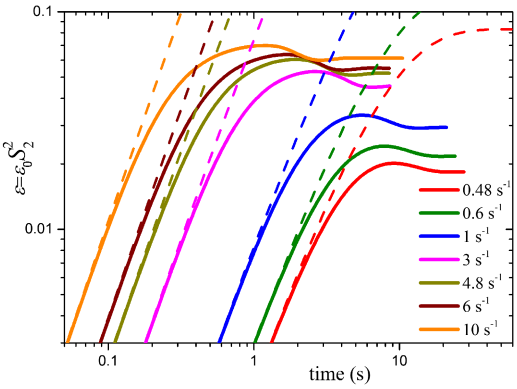

FIG. 3. The transient link-tension coefficient, $\varepsilon = \varepsilon_0 S_2^2$, using strictly identical parameters as in Fig. 1; the dotted lines are those obtained from the small shear rate expansion, see Eq. (1).

where

$$\Gamma_1(t) = 12\sum_{\nu=1,odd}^{\infty}\frac{1}{(\nu\pi)^2 K_2}\exp\left(-K_2\frac{t}{\lambda}\right), \tag{2}$$

and then by expanding $\Gamma_1(t)$ at small times we get $\varepsilon \approx \frac{9}{75}\varepsilon_0(\dot\gamma t)^2$. K_2 is defined in the supplementary material.

As noted in Fig. 1, the tumbling-snake model bears the sufficient capacity to predict $\eta(t)$: at small $\dot\gamma$, it predicts a monotonic approach to the steady-state viscosity η following the overshoot, whereas at larger $\dot\gamma$, an undershoot appears which deepens and moves towards smaller times as the shear rate increases. The position of both the undershoot and the overshoot is seen to agree well with the experimental data. Such a behavior is possible only when $\varepsilon' > 0$ whereas the non-tumbling limit ($\varepsilon' = 0$) always predicts a monotonic approach to η after the overshoot (see Fig. 4 of Ref. 24). This clearly suggests that the origin of the undershoot is the additional rotational diffusion term in the FP equation which enhances the occurrence of tumbling.

This will be more pronounced at large shear rates since the tangent unit vector $\mathbf{u}$, at any position along the chain, will then reside close to the shearing plane, and the random rotational Brownian forces will be sufficient to force it to start a tumbling cycle after residing in a flow-aligned state during a short period only. Tumbling arises much more naturally in the tumbling-snake model, compared to other treatments, through the rotational Brownian term. Note that the prediction of undershoots is possible even for a constant ε; the use of $\varepsilon \sim S_2^2$ is relevant for correcting both the LVE behavior at small times and the violation of the stress-optic law close to equilibrium.

For $\Psi_1(t)$, the tumbling-snake model predicts no undershoots in accord with the experimental measurements (Fig. 2(a)) and it also captures the steady-state values Ψ_1 [see also Fig. S2(b) of the supplementary material]. Similarly, the tumbling-snake model captures the steady-state Ψ_2, within statistical uncertainty [see also Fig. S2(c) of the supplementary material], and again predicts no undershoots (Fig. 2(b)). It should be emphasized that the non-tumbling model ($\varepsilon' = 0$) predicts for both viscometric functions a strictly monotonic approach towards the steady-state value following the overshoot (see Figs. 5 and 6 of Ref. 24).

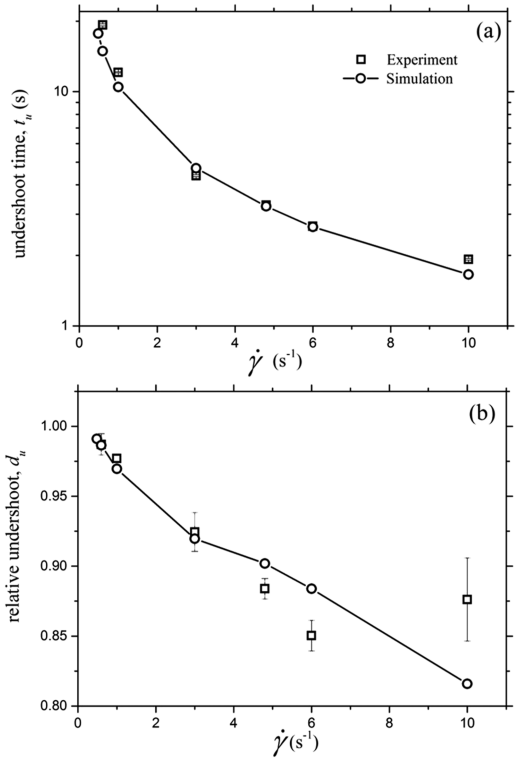

FIG. 4. Comparison between experimental data (squares) and the predictions of the tumbling-snake model (circles connected by lines) for (a) the undershoot time, t_u, and (b) the relative undershoot depth (undershoot depth divided by steady-state value), d_u. Both quantities are obtained from the transient $\eta(t)$ and shown as a function of shear rate $\dot{\gamma}$ (error bars smaller than symbol sizes are omitted).

To come up with quantitative measures, we explored more closely the tumbling-snake model predictions for the position and the depth of the undershoot in $\eta(t)$. The time at which the undershoot occurs, t_u, is depicted in Fig. 4(a) where we note that the tumbling-snake model is capable of predicting t_u quantitatively. We further observe a quantitative agreement of the tumbling-snake prediction for the relative undershoot depth, d_u [Fig. 4(b)], except for the largest rate.

When elongational flows are considered, such a damped oscillatory behavior should be absent from all observables as these flows have no rotational component. A useful constitutive model should bear evidence of this feature without any further readjustments. Indeed, by using parameters as those mentioned above in startup shear, the tumbling-snake model does predict the absence of a damping behavior in the transient uniaxial elongational viscosity (results not shown). Thus, its use in mixed flows poses no additional complication.

In light of these findings, the present work stands as a call to the scientific community to take a closer look into the tumbling-snake model and to consider it as a possible framework for further refinement in the future. It has shown the necessary capacity to predict undershoots in startup shear flow. Further, it can readily be solved using simple BD algorithms for homogenous flows[26,36] and thus also be used in numerical simulations of inhomogeneous flows through the CONNFFESSIT or related approaches.[36,39,40]

See supplementary material for additional details about the polymer solution, comparison with the LVE and steady-state experimental data, and the derivation of the shear relaxation modulus and the LVE dynamic behavior of all material function for the tumbling-snake model.

This work was co-funded by the Republic of Cyprus through the Research Promotion Foundation (Project No. KOYLTOYRA/BP-NE/0415/01) granted to P.S.S. through the Cyprus Research Award-Young Researcher 2015.

[1]M. Doi and S. F. Edwards, J. Chem. Soc., Faraday Trans. 2 **74**, 1789 (1978).
[2]M. Doi and S. F. Edwards, *The Theory of Polymer Dynamics* (Clarendon, Oxford, 1986).
[3]P. G. de Gennes, J. Chem. Phys. **55**, 572 (1971).
[4]H. Watanabe, Prog. Polym. Sci. **24**, 1253 (1999).
[5]T. C. B. McLeish, Adv. Phys. **51**, 1379 (2002).
[6]M. Kröger, Comput. Phys. Commun. **168**, 209 (2005).
[7]K. N. Foteinopoulou, N. C. Karayiannis, V. G. Mavrantzas, and M. Kröger, Macromolecules **39**, 4207 (2006).
[8]C. Tzoumanekas and D. N. Theodorou, Macromolecules **39**, 4592 (2006).
[9]S. H. Jeong, J. M. Kim, J. Yoon, C. Tzoumanekas, M. Kröger, and C. Baig, Soft Matter **12**, 3770 (2016).
[10]P. S. Stephanou, C. Baig, G. Tsolou, V. G. Mavrantzas, and M. Kröger, J. Chem. Phys. **132**, 124904 (2010).
[11]C. Baig and V. G. Mavrantzas, Soft Matter **6**, 4603 (2010).
[12]C. Baig, P. S. Stephanou, G. Tsolou, V. G. Mavrantzas, and M. Kröger, Macromolecules **43**, 8239 (2010).
[13]J. Qin, S. T. Milner, P. S. Stephanou, and V. G. Mavrantzas, J. Rheol. **56**, 707 (2012).
[14]P. S. Stephanou, C. Baig, and V. G. Mavrantzas, Macromol. Theory Simul. **20**, 752 (2011).
[15]P. S. Stephanou, C. Baig, and V. G. Mavrantzas, Soft Matter **7**, 380 (2011).
[16]P. S. Stephanou and V. G. Mavrantzas, J. Non-Newtonian Fluid Mech. **200**, 111 (2013).
[17]P. S. Stephanou and V. G. Mavrantzas, J. Chem. Phys. **140**, 214903 (2014).
[18]M. Doi and S. F. Edwards, J. Chem. Soc., Faraday Trans. 2 **74**, 1802 (1978).
[19]M. Doi and S. F. Edwards, J. Chem. Soc., Faraday Trans. 2 **74**, 1818 (1978).
[20]M. Doi and S. F. Edwards, J. Chem. Soc., Faraday Trans. 2 **75**, 38 (1979).
[21]R. B. Bird, R. C. Armstrong, and O. Hassager, *Dynamics of Polymeric Liquids: Volume 2, Kinetic Theory* (John Wiley & Sons, New York, 1987).
[22]C. F. Curtiss and R. B. Bird, J. Chem. Phys. **74**, 2016 (1981).
[23]C. F. Curtiss and R. B. Bird, J. Chem. Phys. **74**, 2026 (1981).
[24]R. B. Bird, H. H. Saab, and C. F. Curtiss, J. Chem. Phys. **77**, 4747 (1982).
[25]R. B. Bird, H. H. Saab, and C. F. Curtiss, J. Phys. Chem. **86**, 1102 (1982).
[26]P. S. Stephanou and M. Kröger, J. Chem. Phys. **144**, 124905 (2016).
[27]H. H. Saab, R. B. Bird, and C. F. Curtiss, J. Chem. Phys. **77**, 4758 (1982).
[28]M. Kröger, *Models for Polymeric and Anisotropic Liquids* (Springer, Berlin, 2005).
[29]D. Auhl, J. Ramirez, A. E. Likhtman, P. Chambon, and C. Fernyhough, J. Rheol. **52**, 801 (2008).
[30]S. Costanzo, Q. Huang, G. Ianniruberto, G. Marrucci, O. Hassager, and D. Vlassopoulos, Macromolecules **49**, 3925–3935 (2016).
[31]J. Fang, M. Kröger, and H. C. Öttinger, J. Rheol. **44**, 1293 (2000).
[32]M. H. N. Sefiddashti, B. J. Edwards, and B. Khomami, J. Rheol. **59**, 119 (2015).
[33]J. M. Kim and C. Baig, Sci. Rep. **6**, 19127 (2016).
[34]S. R. Strand, S. Kim, and S. J. Karrila, J. Non-Newtonian Fluid Mech. **24**, 311 (1987).
[35]T. Schweizer, J. Hostettler, and F. Mettler, Rheol. Acta **47**, 943 (2008).
[36]H. C. Öttinger, *Stochastic Processes in Polymeric Fluids: Tools and Examples for Developing Simulation Algorithms* (Springer, Berlin, 1996).
[37]R. G. Larson, *Constitutive Equations for Polymer Melts and Solutions* (Butterworth-Heinemann, 1987).
[38]C. Luap, C. Müller, T. Schweizer, and D. Venerus, Rheol. Acta **45**, 83 (2005).
[39]M. Laso and H. C. Öttinger, J. Non-Newtonian Fluid Mech. **47**, 1 (1993).
[40]K. Feigl, M. Laso, and H. C. Öttinger, Macromolecules **28**, 3261 (1995).